PROCEEDINGS OF SCIENCE

Top quark pair production cross section and properties of the top quark in $p\bar{p}$ collisions at $\sqrt{s} = 1.96$ TeV

Christian Schwanenberger[*†]

The University of Manchester, School of Physics & Astronomy, United Kingdom

E-mail: `schwanen@fnal.gov`

An overview over measurements of top quark pair production in $p\bar{p}$ collisions at a center-of-mass energy of $\sqrt{s} = 1.96$ TeV is given. Emphasis is given to measurements of the $t\bar{t}$ cross section in lepton+jets and dilepton final states with up to 5.4 fb^{-1} of integrated luminosity. Examples of measurements of top quark properties such as a measurement of the top quark branching ratio, a search for flavor changing neutral current couplings in top quark decays and an extraction of the top quark pole and $\overline{\text{MS}}$ mass using the $t\bar{t}$ cross section are presented.

The 2011 Europhysics Conference on High Energy Physics-HEP 2011,
July 21-27, 2011
Grenoble, Rhône-Alpes France

[*]Speaker.
[†]on behalf of the D0 Collaboration.

 http://pos.sissa.it/

PoS(EPS-HEP2011)345

1. Introduction

The top quark was discovered in 1995 by the CDF and D0 Collaborations at the Tevatron [1] as the most recent member of the known families of quarks. The existence of the top quark was predicted by theory, but the final proof that the observed particle is indeed the one predicted by the Standard Model (SM) is still required. Therefore, it is essential to investigate top quark properties in great detail and to confront the measurements with theory predictions in order to explore whether the top quark is connected to new physics.

In this presentation high-precision measurements of various essential properties such as the $t\bar{t}$ production rate, the top quark decay couplings and the top quark mass are presented and compared to SM predictions. The analyses are based on data collected with the D0 detector in Run II of the Fermilab Tevatron Collider with an integrated luminosity of up to 5.4 fb^{-1}.

2. Top quark pair production cross section

The inclusive $t\bar{t}$ production cross section ($\sigma_{t\bar{t}}$) is predicted in the SM with a precision of 6% to 8% [2, 3, 4]. Due to the large mass of the top quark, many models of physics beyond the SM predict observable effects in the top quark sector which can affect the top quark production rate. For example, the decay of a top quark into a charged Higgs boson and a b quark ($t \to H^+b$) would affect the value of $\sigma_{t\bar{t}}$ extracted from different final states [5]. In the SM, the top quark decays with almost 100% probability into a W boson and a b quark.

We have performed a new measurement of the inclusive top quark production cross section in the lepton+jets (ℓ+jets) final state [6] where one of the W bosons from the top quark decays hadronically into a $q\bar{q}'$ pair and the other leptonically into $e\nu_e$, $\mu\nu_\mu$, or $\tau\nu_\tau$. We consider both direct electron and muon decays, as well as secondary electrons and muons from τ decay. The data samples are enriched in $t\bar{t}$ events by requiring more than one jet of high transverse momentum, one isolated high-p_T electron or muon and large missing transverse energy. The b-jets are identified using a neural network (NN) formed by combining variables characterizing the properties of secondary vertices and of tracks with large impact parameters relative to the PV [7].

We measure the $t\bar{t}$ production cross section using three methods: (i) A "kinematic" method based on $t\bar{t}$ event kinematics where we use final states with 2, 3 or >3 jets. To distinguish $t\bar{t}$ signal from background, we construct a multivariate discriminant that exploits differences between kinematic properties of $t\bar{t}$ ℓ+jets signal and the dominant $W+$jets background. (ii) A "counting" method using b-jet identification where we use final states with exactly three jets and more than three jets and further separate each channel into events with 0, 1, and >1 b-tagged jets. The fit of the $t\bar{t}$ cross section to data is performed simultaneously with determining the heavy flavor fraction for $W+$jet processes using a binned maximum likelihood fit for the predicted number of events, which depends on $\sigma_{t\bar{t}}$. (iii) A method utilizing both techniques, referred to as the "combined" method where kinematic information and b-jet identification are used. We split the selected sample into events with 2, 3, and >3 jets and into 0, 1, and >1 b-tagged jets. Events with >2 jets but no b-tagged jet are dominated by background. For these events and also for events with three jets and one b-tag we construct a discriminant. For all other subchannels the signal purity is already high and therefore we do not form discriminants.

PoS(EPS-HEP2011)345

We have also performed a new measurement in the dilepton ($\ell\ell$) final state [8] where both W bosons coming from $t \to Wb$ decay leptonically. Final states with at least two jets and two leptons (ee, $e\mu$, $\mu\mu$), and events with one jet for the $e\mu$ final state were considered. In order to achieve a better separation between signal and background, we use the distribution of the smaller b-tagging NN output [7] of the two leading jets.

Table 1: Measured $t\bar{t}$ cross section for all three methods for ℓ+jets and dilepton channels. The first quoted uncertainty denotes the statistical, the second the systematic contribution.

Method	ℓ+jets kinematic	ℓ+jets counting	ℓ+jets combined	dilepton
$\sigma_{t\bar{t}}$ [pb]	$7.68 \pm 0.31^{+0.64}_{-0.56}$	$8.13 \pm 0.25^{+0.99}_{-0.86}$	$7.78 \pm 0.25^{+0.73}_{-0.59}$	$8.05^{+0.50\,+1.05}_{-0.48\,-0.97}$

Table 1 summarizes the measurements in the ℓ+jets channel for the three different methods and in the $\ell\ell$ channel for a top quark mass of 172.5 GeV. All our results are consistent with the theoretical predictions of $\sigma_{t\bar{t}} = 6.41^{+0.51}_{-0.42}$ pb [2] and $\sigma_{t\bar{t}} = 7.46^{+0.48}_{-0.67}$ pb [3], and they agree with the result from the CDF Collaboration [9]. The ℓ+jets cross section derived using the "combined" method was combined with the cross section measured in the dilepton channel yielding

$$\sigma_{t\bar{t}} = 7.56^{+0.63}_{-0.56}\,(\mathrm{stat}+\mathrm{syst}+\mathrm{lumi})\,\mathrm{pb}.$$

The relative precision of 8% is comparable to the theoretical calculations.

3. Top quark decay couplings

In the SM the decay rate of the top quark into a W boson and a down-type quark q ($q = d,s,b$) is proportional to $|V_{tq}|^2$, the squared element of the Cabibbo Kobayashi Maskawa (CKM) matrix. Under the assumption of a unitary 3×3 CKM matrix, $|V_{tb}|$ is indirectly constrained to $|V_{tb}| = 0.999152^{+0.000030}_{-0.000045}$ [10], and the top quark decays almost exclusively to Wb. The existence of new physics in top quark decays such as due to anomalous couplings or due to a fourth generation of quarks would remove this constraint and accommodate significantly smaller values of $|V_{tb}|$. In the following two investigations of the coupling involved in top quark decays are presented.

3.1 Measurement of the ratio $\mathscr{B}(t\to Wb)/\mathscr{B}(t\to Wq)$

We have measured the ratio of top quark branching fractions $R = \mathscr{B}(t\to Wb)/\mathscr{B}(t\to Wq)$, where q can be a d, s or b quark, in the ℓ+jets and $\ell\ell$ $t\bar{t}$ final states [11]. Using NN b-tagging we distinguish between the standard decay mode of the top quark $t\bar{t} \to W^+bW^-\bar{b}$ (indicated by bb), and decay modes that include light quarks ($q_l = d,s$): $t\bar{t} \to W^+bW^-\bar{q}_l$ (bq_l) and $t\bar{t} \to W^+q_lW^-\bar{q}_l$ (q_lq_l). In the ℓ+jets channel we use the "combined" method and in the $\ell\ell$ channel the NN discriminant as described in Sect. 2 to extract R. We perform a maximum likelihood fit to data utilizing templates for the decay modes bb, bq_l, q_lq_l for $t\bar{t}$ as well as for all background components. Figures 1 (left) and (middle) show the number of b-tagged jets in ℓ+3 jets and ℓ+$\geq$3 jets events, respectively, for data and simulation for $R=0$, $R=0.5$ and $R=1$. Figure 1 (right) compares the distributions of the NN discriminant for predicted and observed events in the combined $\ell\ell$ final state. Fitting simul-

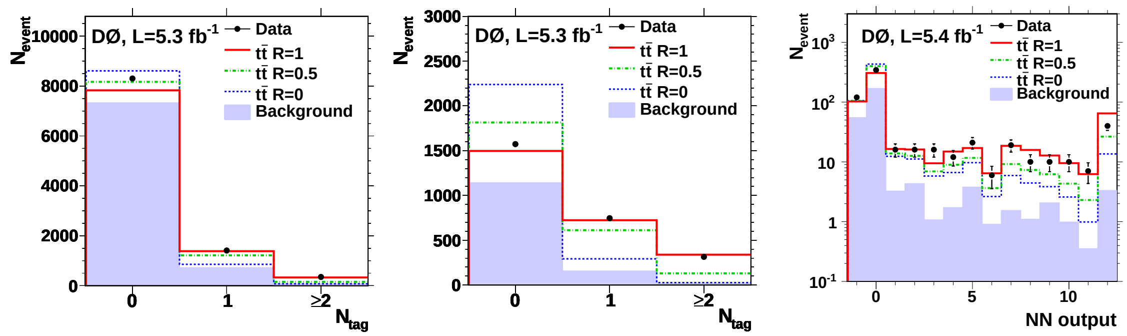

Figure 1: Number of b-tagged jets in ℓ+jets events with three jets (left) and at least four jets (middle). (Right) Distribution in the minimum b-tag NN output of the jets of highest-p_T for dilepton final states.

taneously all channels in the $\ell\ell$ and ℓ+jets final states, we measure $R = 0.90 \pm 0.04\,(\mathrm{stat}+\mathrm{syst})$. This agrees within approximately 2.5 standard deviations with the SM prediction of R close to one and is the most precise determination of R to date. Assuming the unitarity of the CKM matrix, we extract the interval at 95% CL on the element $|V_{tb}|$ as 0.90–0.99.

3.2 Search for flavor changing neutral currents in decays of top quarks

Flavor changing neutral currents (FCNC) allow for transitions between quarks of different flavor but same electric charge [12]. FCNC are sensitive indicators of new physics, because they are suppressed in the SM. Here we present a search for flavor changing neutral currents in decays of top quarks using 4.1 fb^{-1} of integrated luminosity [13]. We analyze $t\bar{t}$ production, where either one or both of the top quarks decay via $t \to Zq$ ($q = u, c$) or their charge conjugates. Any top quark that does not decay via $t \to Zq$ is assumed to decay via $t \to Wb$. We investigate channels where the W and Z bosons decay leptonically. The u, c, and b quarks subsequently hadronize, giving rise to a final state with three charged leptons ($\ell = e, \mu$), an imbalance in momentum transverse to the $p\bar{p}$ collision axis ($\not{E}_T$, from the escaping neutrino in the $W \to \ell\nu$ decay), and jets. We consider four independent decay signatures: $eee + \not{E}_T + X$, $ee\mu + \not{E}_T + X$, $\mu\mu e + \not{E}_T + X$, and $\mu\mu\mu + \not{E}_T + X$, where X is any number of jets, $n_{\rm jet}$.

To achieve better separation between signal and background, we analyze the $n_{\rm jet}$ and $H_{\rm T}$ distributions (defined as the scalar sum of transverse momenta of all leptons, jets, and $\not{E}_T$), and the reconstructed invariant mass for the products of the decay $t \to Zq$. FCNC $t\bar{t}$ production leads to larger jet multiplicities and also a larger $H_{\rm T}$. This is shown in Fig. 2 (left). The $m_{\rm t}^{\rm reco}$ distribution is shown in Fig. 2 (middle). None of the investigated observables show evidence for the presence of FCNC in the decay of $t\bar{t}$. We therefore set a 95% C.L. limit on the branching ratio $B(t \to Zq) < 3.2\%$, which is currently the world's best limit. This limit is converted to limits on the FCNC vector, v_{tqZ}, and axial vector, a_{tqZ}, couplings yielding $v_{tqZ} < 0.19$ at the 95% C.L. for $m_t = 172.5$ GeV. Figure 2 (right) shows current limits from experiments at the LEP, HERA, and Tevatron colliders as a function of the FCNC couplings $\kappa_{tu\gamma}$ (defined in Ref. [12]) and v_{tuZ} for $m_t = 175$ GeV.

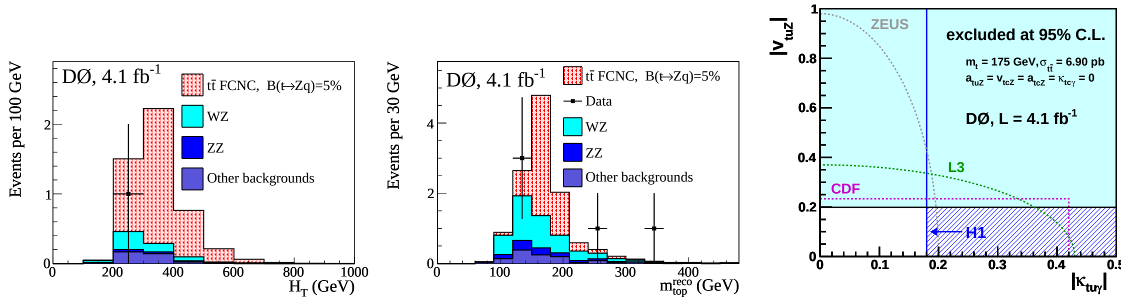

Figure 2: $H_{\rm T}$ (left) and $m_{\rm t}^{\rm reco}$ (right) distributions of data, FCNC $t\bar{t}$ signal, and expected background for events with $n_{\rm jet} \geq 2$ (left) and $n_{\rm jet} \geq 1$ (middle). Right: Upper limits at the 95% C.L. on the anomalous $\kappa_{tu\gamma}$ and v_{tuZ} couplings assuming $m_t = 175$ GeV. The domain excluded by D0 is represented by the light (blue) shaded area. The hatched area corresponds to the additional domain excluded at HERA by the H1 experiment [14]. Also shown are upper limits obtained at LEP by the L3 experiment [15] (green dashed), at HERA by the ZEUS experiment [16] (grey dashed), and at the Tevatron by the CDF experiment [17] (magenta dashed). The region above or to the right of the respective lines is excluded.

4. Top quark mass

The mass of the top quark (m_t) has been measured with a precision of 0.6%, and its current Tevatron average value is $m_t = 173.3 \pm 1.1$ GeV [18]. Beyond leading-order quantum chromodynamics (LO QCD), the mass of the top quark is a convention-dependent parameter. Therefore, it is important to know how to interpret this experimental result in terms of renormalization conventions [19] if the value is to be used as an input to higher-order QCD calculations or in fits of electroweak precision observables and the resulting indirect Higgs boson mass bounds [20].

Current MC simulations are performed in LO QCD, and higher order effects are simulated through parton showers at modified leading logarithms (LL) level. In principle, it is not possible to establish a direct connection between the mass definition as implemented in MC simulations $m_t^{\rm MC}$, and any other mass scheme, such as the pole or $\overline{\rm MS}$ mass scheme, without calculating the parton showers to at least next-to-leading logarithms (NLL) accuracy. However, it has been argued that $m_t^{\rm MC}$ should be close to the pole mass [21]. The relation between $m_t^{\rm MC}$ and the top quark pole mass ($m_t^{\rm pole}$) or $\overline{\rm MS}$ mass ($m_t^{\overline{\rm MS}}$) is still under theoretical investigation. In calculations such as in Ref. [20] it is assumed that $m_t^{\rm MC}$ measured at the Tevatron is equal to $m_t^{\rm pole}$.

Here we extract the pole mass $m_t^{\rm pole}$, and the $\overline{\rm MS}$ mass at the scale of the $\overline{\rm MS}$ mass, $m_t^{\overline{\rm MS}}(m_t^{\overline{\rm MS}})$, comparing the measured inclusive $t\bar{t}$ production cross section $\sigma_{t\bar{t}}$ with fully inclusive calculations at higher-order QCD that involve an unambiguous definition of m_t and compare our results to $m_t^{\rm MC}$ [22]. This extraction provides an important test of the mass scheme as applied in MC simulations and gives complementary information, with different sensitivity to theoretical and experimental uncertainties than the direct measurements of $m_t^{\rm MC}$ that rely on kinematic details of the mass reconstruction. We use the measurement of $\sigma_{t\bar{t}}$ in the lepton+jets channel using the "counting" method [6] , calculate likelihoods for $\sigma_{t\bar{t}}$ as a function of m_t, and use higher-order QCD predictions based on the pole-mass or the $\overline{\rm MS}$-mass conventions to extract $m_t^{\rm pole}$or $m_t^{\overline{\rm MS}}$, respectively.

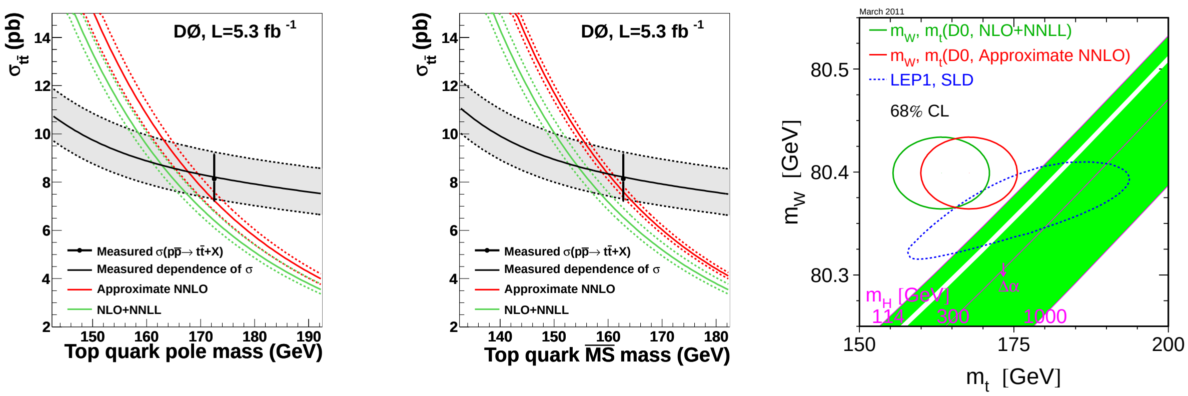

Figure 3: (Color online) Measured $\sigma_{t\bar{t}}$ and theoretical NLO+NNLL [2] and approximate NNLO [3] calculations of $\sigma_{t\bar{t}}$ as a function of $m_t^{\rm pole}$ (left) and as a function of $m_t^{\overline{\rm MS}}$ (middle), assuming that $m_t^{\rm MC} = m_t^{\rm pole}$. The colored dashed lines represent the uncertainties for the two theoretical calculations from the choice of the PDF and the renormalization and factorization scales (added quadratically). The point shows the measured $\sigma_{t\bar{t}}$ for $m_t^{\rm MC} = 172.5$ GeV, the black curve is the fit to the mass dependence, and the gray band corresponds to the total experimental uncertainty. Right plot: Constraints on the W boson mass from the LEP-II/Tevatron experiments and the top quark pole mass extracted from the $t\bar{t}$ cross section in NLO+NNLL [2] (green contour) and approximate NNLO [3] (red contour). This is compared to the indirect constraints on the W boson mass and the top quark mass based on LEP-I/SLD data (dashed contour). In both cases the 68% CL contours are given. Also shown is the SM relationship for the masses as a function of the Higgs mass in the region favored by theory (<1000 GeV) and not excluded by direct searches (114 GeV to 158 GeV and >173 GeV). The arrow labelled $\Delta\alpha$ shows the variation of this relation if $\alpha(m_Z^2)$ is varied between -1 and $+1$ sd. This variation gives an additional uncertainty to the SM band shown in the figure.

Fig. 3 (left) shows the parameterization of the measured and the predicted $\sigma_{t\bar{t}}(m_t^{\rm pole})$ [2, 3]. The extracted value of $m_t^{\rm pole}$ using the approximate NNLO calculation [3] is $167.5^{+5.2}_{-4.7}$ GeV. Calculations of the $t\bar{t}$ cross section [2, 3] have also been performed as a function of $m_t^{\overline{\rm MS}}$ leading to a faster convergence of the perturbative expansion [3]. Therefore, comparing the dependence of the measured $\sigma_{t\bar{t}}$ to theory as a function of m_t provides an estimate of $m_t^{\overline{\rm MS}}$ which benefits from a higher perturbative stability compared to the extraction of $m_t^{\rm pole}$. We note that a previous extraction of $m_t^{\overline{\rm MS}}$ [3] ignored the m_t dependence of the measured $\sigma_{t\bar{t}}$. Figure 3 (middle) shows the measured $\sigma_{t\bar{t}}$ as a function of $m_t^{\overline{\rm MS}}$, together with the calculations [2, 3]. The results for the extracted value of $m_t^{\overline{\rm MS}}$ for the approximate NNLO calculation [3] is $160.0^{+4.8}_{-4.3}$ GeV. The Tevatron direct measurements of m_t are consistent with both $m_t^{\rm pole}$ measurements within 2 sd, but they are different by more than 2 sd from the extracted $m_t^{\overline{\rm MS}}$. The results on $m_t^{\rm pole}$ and their interplay with other electroweak results within the SM are displayed in Fig. 3 (right), which is based on Ref. [20]. For the first time, $m_t^{\overline{\rm MS}}$ is extracted with the m_t dependence of the measured $\sigma_{t\bar{t}}$ taken into account. Our measurements favor the interpretation that the Tevatron m_t measurements based on reconstructing top quark decay products is closer to the pole than to the $\overline{\rm MS}$ top quark mass.

5. Conclusions

Recent measurements of the top quark pair production cross section, top quark decay couplings and the top quark pole and $\overline{\mathrm{MS}}$ mass have been presented. For all investigations performed in various final states analyzing many different observables, we observe good agreement with the SM predictions. There are still excellent prospects for top quark physics at the Tevatron collider since including the full Run ll data will double the statistics for the analyses presented here.

References

[1] F. Abe *et al.* (CDF Collaboration), Phys. Rev. Lett. **74**, 2626 (1995); S. Abachi *et al.* (DØ Collaboration), Phys. Rev. Lett. **74**, 2632 (1995).

[2] V. Ahrens, A. Ferroglia, M. Neubert, B. D. Pecjak, and L. L. Yang, J. High Energy Phys. **09**, 097 (2010); V. Ahrens, A. Ferroglia, M. Neubert, B. D. Pecjak, and L. L. Yang, Nucl. Phys. Proc. Suppl. **205-206**, 48 (2010).

[3] S. Moch and P. Uwer, Phys. Rev. D **78**, 034003 (2008); U. Langenfeld, S. Moch, and P. Uwer, Phys. Rev. D **80**, 054009 (2009); M. Aliev *et al.*, Comput. Phys. Commun. **182**, 1034 (2011).

[4] N. Kidonakis, Phys. Rev. D **82**, 114030 (2010).

[5] V. M. Abazov *et al.* [D0 Collaboration], Phys. Rev. D **80**, 071102(R) (2009); V. M. Abazov *et al.* [D0 Collaboration], Phys. Lett. B **682**, 278 (2009); A. Abulencia *et al.* [CDF Collaboration], Phys. Rev. Lett. **96**, 042003 (2006).

[6] V. M. Abazov *et al.* [D0 Collaboration], Phys. Rev. D **84**, 012008 (2011).

[7] V. M. Abazov *et al.* [D0 Collaboration], Nucl. Instrum. Methods Phys. Res. A **620**, 490 (2010).

[8] V. M. Abazov *et al.* [D0 Collaboration], Phys. Lett. B **704**, 403 (2011).

[9] T. Aaltonen *et al.* [CDF Collaboration], Phys. Rev. Lett. **105**, 012001 (2010).

[10] K. Nakamura et al. (Particle Data Group), J. Phys. G **37**, 075021 (2010).

[11] V. M. Abazov *et al.* [D0 Collaboration], Phys. Rev. Lett. **107**, 121802 (2011).

[12] T. Han and J. L. Hewett, Phys. Rev. D **60**, 074015 (1999).

[13] V. M. Abazov *et al.* [D0 Collaboration], Phys. Lett. B **701**, 313 (2011).

[14] F. D. Aaron *et al.* [H1 Collaboration], Phys. Lett. B **678**, 450 (2009).

[15] P. Achard *et al.* [L3 Collaboration], Phys. Lett. B **549**, 290 (2002);

[16] S. Chekanov *et al.* [ZEUS Collaboration], Phys. Lett. B **559**, 153 (2003).

[17] F. Abe *et al.*, Phys. Rev. Lett. **80**, 2525 (1998); T. Aaltonen *et al.* [CDF Collaboration], Phys. Rev. Lett. **101**, 192002 (2008).

[18] CDF and D0 Collaborations, arXiv:1007.3178 [hep-ex].

[19] A. H. Hoang, A. Jain, I. Scimemi and I. W. Stewart, Phys. Rev. Lett. **101**, 151602 (2008).

[20] ALEPH, CDF, D0, DELPHI, L3, OPAL, and SLD Collaborations, LEP Electroweak Working Group, Tevatron Electroweak Working Group, SLD Electroweak Working Group, and SLD Heavy Flavour Group, arXiv:1012.2367 [hep-ex].

[21] S. Fleming, A. H. Hoang, S. Mantry and I. W. Stewart, Phys. Rev. D **77**, 074010 (2008).

[22] V. M. Abazov *et al.* [D0 Collaboration], Phys. Lett. B **703**, 422 (2011).